

Chapter 48

Super Sparse Projection Reconstruction of Computed Tomography Image Based-on Reweighted Total Variation

Gongxian Liu and Jianhua Luo

Abstract Sparse projection is an effective way to reduce the exposure to radiation during X-ray CT imaging. However, reconstruction of images from sparse projection data is challenging. In this paper, a novel method called reweight total variation (WTV) is applied to solve the challenging problem. And based on WTV, an iteration algorithm which allows the image to be reconstructed accurately is also proposed. The experimental results on both simulated and real images have consistently shown that, compared to the popular total variation (TV) method and the classical Algebra Reconstruction Technique (ART), the proposed method achieves better results when the projection is sparse, and performs comparably with TV and ART when the number of projections is relatively high. Therefore, the application of the proposed reconstruction algorithm may permit reduction of the radiation exposure without trade-off in imaging performance.

Keywords Sparse Projection Reconstruction · CT · Reweight total variation · Iterative Reconstruction

48.1 Introduction

X-ray computed tomography (CT) has played an important role in medical field. Nonetheless, exposing in strong X-ray intensity for a long time will do harm to people's health. An effective way to achieve the reduction of the radiation

G. Liu (✉)

School of Biomedical Engineering, Shanghai Jiao Tong University,
Shanghai, China
e-mail: liugxian2006@gmail.com

J. Luo

School of Aeronautics and Astronautics, Shanghai Jiao Tong University,
Shanghai, China

exposure is to reduce the number of projections required for reconstructing the image, but the image reconstructed from sparse projections often suffers from serious problems, such as blurring and artifacts.

Various algorithms have been developed to reconstruct image from sparse projections. There are mainly two methods, i.e., interpolating the missing data which is followed by image analytic reconstruction and iterative reconstruction. Numerous iterative algorithms have been developed for tomography image reconstruction. Among these algorithms mentioned, the widely used iterative algorithms for tomography imaging are the algebraic reconstruction technique (ART) and the expectation–maximization (EM) Algorithm. These methods differ in the constraints exposed on the image and the cost function that to be minimized [1]. Furthermore, they will result in artifacts as the projections reduce. For the case where the data is consistent yet is not sufficient to determine a unique solution to the imaging model, the ART algorithm finds the image that is consistent with the data and minimizes the sum-of-squares of the image pixel values [2]. In this paper, TV [3] and WTV [4] are introduced to reconstruct tomography images with super sparse projections. The two methods are actually iterative methods that differ in the cost function. WTV is a novel method for sparse image recovery and substantially less measurement is needed for exact recovery. It is a method that adds weights to TV, i.e., large coefficients in TV are penalized heavily than small coefficients [5].

The organization of this paper is as follows. Firstly, central slice theory and the main theory of TV and WTV are introduced in Sect. 48.2. Based on the theories mentioned in Sect. 48.2, experiments on both simulated images and real images are devised in Sect. 48.3. Finally, the conclusions are drawn and the future work is discussed in Sect. 48.4.

48.2 Theories

48.2.1 Central Slice Theory

The central slice theory is that if projecting an image to a line and doing a Fourier transform of the projection, it is equivalent to doing a two-dimensional Fourier transform to the image first and slicing through the original in the orthogonal direction. Then sparse projections can be converted into sparse radial spectral data according to the Fourier slice theorem. The Fourier transform of a parallel beam projection gives a slice of the two-dimensional (2-D) Fourier transform. Given an image, M projections in the image space are equivalent to sampling M radial lines of the image's spectrum, thus generating sparsely sampled radial spectral data. The smaller M is, the sparser the radial spectral data will be. Therefore, M is also referred to as sparse level of projections [6]. As Fig. 48.1 shows, suppose that there are 30 projections in the image domain, it is equivalent to getting data in the orthogonal directions in Fourier domain.

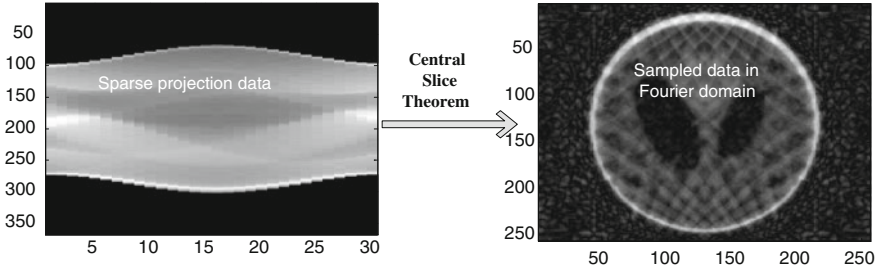


Fig. 48.1 Projection in image space is transformed to Fourier domain based on central slice theorem

48.2.2 Total Variation and Reweight Total Variation

Since CT image has a sparse or nearly sparse gradient, it is meaningful to search for the reconstruction with minimal TV norm, i.e.,

$$\min \|x\|_{TV} \quad s.t \quad y = \Phi x \tag{48.1}$$

In Eq. (48.1), $x_{n \times n}$ is the image to be reconstructed and $\Phi_{n \times n}$ is the measurement matrix which is defined as $\Phi = MF$, where $M_{m \times n}$ is the mask matrix that samples data in the image in Fourier domain. The mask matrix is also called radial trace. $F_{n \times n}$ is Fourier masking operator, and $y_{m \times n}$ is the measured data. $\|x\|_{TV}$ is defined in Eq. (48.2):

$$\|x\|_{TV} = \sum_{1 \leq i,j \leq n-1} \sqrt{(x_{i+1,j} - x_{i,j})^2 + (x_{i,j+1} - x_{i,j})^2} = \|Dx\| \tag{48.2}$$

And adding some weights to TV, it will get WTV which is defined as Eq. (48.3)

$$\|x\|_{WTV} = \sum_{1 \leq i,j \leq n-1} W_{i,j} \sqrt{(x_{i+1,j} - x_{i,j})^2 + (x_{i,j+1} - x_{i,j})^2} = \|WDx\| \tag{48.3}$$

where $W_{i,j}$ is the weight of TV, which is defined in Eq. (48.4):

$$W_{i+1}^l = \frac{1}{\|x_{i,j}^l\|_{TV} + \varepsilon} \tag{48.4}$$

In Eq. (48.4), ε is set above zero to provide stability of the algorithm and this will ensure that a zero-valued component in x^ℓ does not strictly prohibit a nonzero estimate at the next step. Empirically, ε should be set slightly smaller than the expected nonzero magnitudes of x . In this paper, $\varepsilon = 0.1$. Then by solving the following equation, the exact reconstruction will be acquired.

$$\min \|x\|_{WTV} \quad s.t \quad y = \Phi x \tag{48.5}$$

Based on the above theory, the main steps of solving WTV are devised in the following.

- Step 1. Set $l = 0$ and $W_{ij}^0 = 1, 1 \leq i, j \leq n$;
- Step 2. Solve the WTV minimization problem, $x^l = \arg \min \sum_{1 \leq i, j \leq n} \|x_{ij}\|_{WTV}$
s.t. $y = \Phi x$;
- Step 3. Update the weights for each $(i, j) 1 \leq i, j \leq n, W_{ij}^{l+1} = \frac{1}{\|x_{ij}^l\|_{TV} + \epsilon}$;
- Step 4. Terminate on convergence or when l gets the max iterations. Otherwise increases l and go to step 2.

A robust quasi-Newton method [7] is used in step 2. Consider Eq. (48.5), the energy functional is given by Eq. (48.6).

$$E(x, \lambda) = \|x\|_{WTV} + \frac{\lambda}{2} \|\Phi x - y\|^2 \quad (48.6)$$

where λ controls the tradeoff between solution sparsity and data fidelity. Then minima of E are yielded as solutions of the associated Euler–Lagrange Eq. (48.7).

$$L(x, \lambda) = \Psi^* \Psi x + \lambda \Phi^* (\Phi x - y) = 0 \quad (48.7)$$

where $\psi = WD$. Then consolidation of the target variable x yields

$$[\Psi^* \Psi + \lambda \Phi^* \Phi] x = \lambda \Phi^* y \quad (48.8)$$

Then robust quasi-Newton iteration is obtained for the computation of x .

$$x^{t+1} = x^t + \Delta^t \quad (48.9)$$

where

$$[\Psi^* \Psi + \lambda \Phi^* \Phi] \Delta^t = -L(x^t, \lambda) \quad (48.10)$$

48.3 Experimental Results

To evaluate the WTV and TV method, digital phantoms from popular Shepp-Logan image and one real image are used. The sparse projections are simulated by generating the specified number of uniformly distributed projections from the phantom and real images. And to evaluate the accuracy of the reconstructed image, we adopt the standard deviation (STD) of errors between the constructed image and reference image.

48.3.1 Measurement of the Accuracy

We consider the constructed image as $x(i,j)$ and the original image as $x_0(i,j)$, the STD is computed in Eq. (48.11).

$$STD = \sqrt{\frac{1}{N^2} \sum_{i=1}^N \sum_{j=1}^N [e(i,j) - \bar{e}]^2} \quad (48.11)$$

where $e(i,j) = x(i,j) - x_0(i,j)$, and $\bar{e} = \frac{1}{N^2} \sum_{i=1}^N \sum_{j=1}^N e(i,j)$. The smaller the STD is, the less the reconstructed error is.

48.3.2 Reconstruction of Phantom Image

The performances of the ART, TV and WTV methods at different sparse level M are evaluated using both noise-free and noisy projections of the Shepp-Logan phantom image. The noisy projections are generated by adding to the noise-free projections zero-mean Gaussian noise with variance 0.0001. Sparse projections are simulated at the sparse levels ranging from 10 to 31 and images are reconstructed using the ART, TV and WTV methods. The experimental results are shown in Fig. 48.2. In Fig. 48.2b, c and d, WTV method can reconstruct the phantom image perfectly with only 10 projections, while image reconstructed by TV method suffers artifacts severely. In Fig. 48.2f, g and h, WTV performs a little better than TV method under noise condition. Notice from Fig. 48.2i, j that the WTV method constantly outperforms the ART and TV methods at all sparse levels in both noise-free and noisy cases. In Fig. 48.2j, The Y-Axis uses semi-log since the STD of WTV is approximate to zero.

48.3.3 Reconstruction of Real Images

To study the performance of TV and WTV methods in reconstructing images with complex structures, 99 axial slices of a real CT brain images (courtesy of North Carolina Memorial Hospital and University of North Carolina, <http://www-graphics.stanford.edu/data/voldata/>) are used. Fig. 48.3 shows the reconstruction results of the 61st slice. A line profile of a pertinent section of each image is shown in Fig. 48.3e, which shows WTV method performs better. Notice from Fig. 48.3f that the WTV method constantly outperforms the ART and TV methods at all sparse levels.

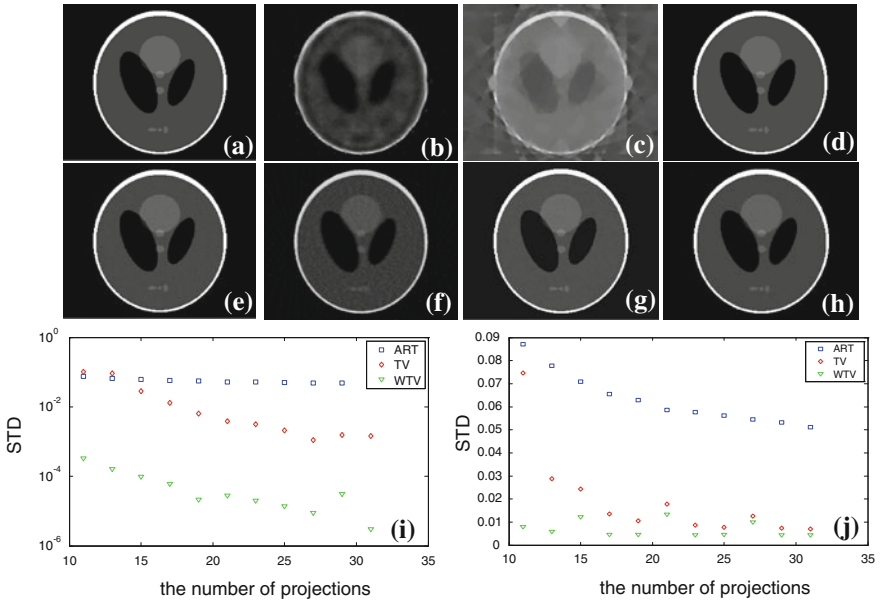


Fig. 48.2 Reconstruction of phantom image. **a** Is the noise-free image; **b**, **c** and **d** are images reconstructed by the ART, TV and WTV methods respectively with 10 projections; **e** is noised image, **f**, **g** and **h** are noised images reconstructed with 30 projections; **i** and **j** shows the STDs between reconstructed image and noise-free or noised image with 11–31 projections, respectively

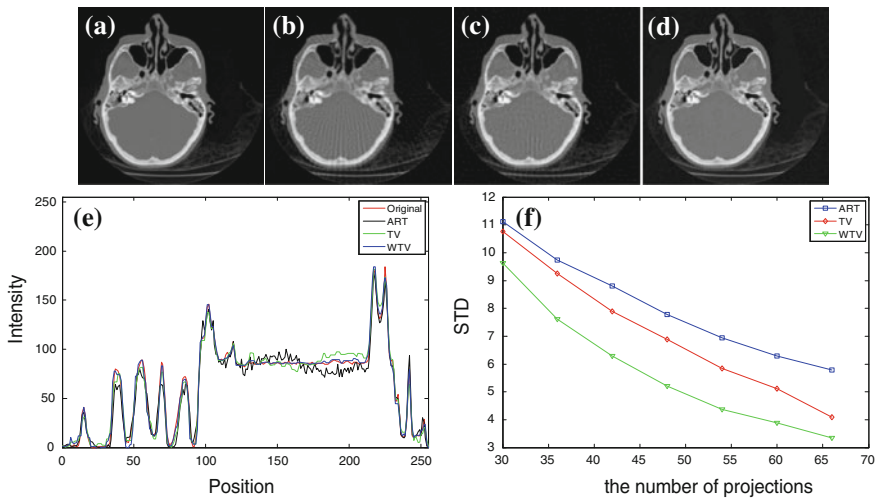


Fig. 48.3 Reconstruction of the slice 61 (brain), in which the number of projections is 66. **a** Is the reference image, **b**, **c** and **d** are the images reconstructed by the ART, TV and WTV methods, respectively. **e** Shows the line profile. **f** Shows the STD between the reference image and reconstructed image using 30–66 projections

48.4 Discussion and Conclusion

Numerical experiment results on both simulated and real data have shown that WTV has a better performance than classical TV method. WTV can reconstruct images more accurately by using fewer projections. As a consequence, the application of WTV method may permit reduction of the radiation exposure without trade-off in imaging performance. However, both methods perform unstably with increasing projections. Initial guess is that sampled data is uniform. And it is difficult to make general conclusions about the performance of WTV algorithm because its performance depends on the structure of the scanned object. During the process of iteration, ε is set to be a fixed value. How to get the best value of ε also needs to be researched. The future work is to search some algorithms to ensure the stability of reconstruction methods and doing more tests about other kinds of CT images. And testing the algorithm with adaptive ε to get the best one is another future task.

References

1. Sidky, E.Y., Kao, C.-M., Pan, X.: Accurate image reconstruction from few-views and limited-angle data in divergent-beam CT. *J X-Ray Sci. Technol.* **14**, 119–139 (2006)
2. Sidky, E.Y., Pan, X.: Image reconstruction in circular cone-beam computed tomography by constrained, total-variation minimization. *Phys. Med. Biol.* **53**, 4777–4807 (2008)
3. Rudin, L.I., Osher, S., Fatemi, E.: Nonlinear total variation based noise removal algorithms. *Phys. D* **60**, 259–268 (1992)
4. Candès, E.J., Wakin, M.B., Boyd, S.P.: Enhancing sparsity by reweighted ℓ_1 minimization. *J. Fourier Anal. Appl.* **14**, 877–905 (2008)
5. Candès, E., Romberg, J., Tao, T.: Robust uncertainty principles: exact signal reconstruction from highly incomplete frequency information. *IEEE Trans. Inf. Theor.* **52**, 489–509 (2006)
6. Luo, J., Liu, J., Li, W., Zhu, Y., Jiang, R.: Image reconstruction from sparse projections using S-transform. *J. Math. Imaging Vision* **43**, 227–239 (2012)
7. Trzasko, J., Manduca, A.: Highly undersampled magnetic resonance image reconstruction via homotopic ℓ_0 -Minimization. *IEEE Trans. Med. Imaging* **28**, 106–112 (2009)